Macromolecules
ARTICLE

*Macromolecules* **2009**, *42*, 8093–8101 **8093**
DOI: 10.1021/ma901434w

# Online Monitoring of Molecular Weight and Other Characteristics during Semibatch Emulsion Polymerization under Monomer Starved and Flooded Conditions

**Alina M. Alb* and Wayne F. Reed**

*Tulane University, New Orleans, Louisiana, 70118*

*Received July 2, 2009; Revised Manuscript Received September 16, 2009*

ABSTRACT: Reaction kinetics in semibatch emulsion polymerization of methyl methacrylate, were monitored by automatic continuous online monitoring of polymerization reactions (ACOMP). Semibatch reagent feed to the reactor at different flow rates allowed the transition between the monomer starved and flooded regimes and the approach to and maintenance of near steady state conditions to be monitored and quantified, and yielded relationships between flow regimes and monomer conversion kinetics, polymer weight-average molecular weight $M_w$, and intrinsic viscosity $[\eta]_w$. Polymer molecular weight distributions together with latex particle size and number play an important role in defining the macroscopic characteristics and performance of polymeric materials. The change in the monomer feed rates during reaction allowed simultaneous influence on and verification of the evolution of these parameters during synthesis. When flow rate changes to the reactor were made it was verified that the characteristic rate of achieving the new pseudosteady state was close to the first order reaction rate. Multidetector size exclusion chromatography was used to cross-check results and measure full distributions of endproducts. Latex polymer size was measured with dynamic light scattering. An important advance for this field is that polymer $M_w$ is determined continuously during the reaction and in an absolute fashion, based on multiangle light scattering detection available.

## Introduction and Background

Semibatch emulsion polymerization is a versatile process which allows polymer latexes with special particle morphology and composition to be produced. Smaller size and narrower particle size distributions than those resulting from batch reactions are obtained through this process making it more suitable to applications in which specific surface area is critically important. In addition to its operational flexibility, the fact that the semibatch emulsion polymerization can easily remove the large amount of heat generated during the reaction makes it a preferred technique. Summary guidelines were formulated in several studies on emulsion polymerization reactions done in batch and semibatch mode under various configurations.[1−9]

Emulsion polymerization in batch generally comprises three stages:[10,11] interval I, in which free radicals generated in the aqueous phase enter micelles and form polymer particles, interval II, where particles grow as they absorb monomer from monomer droplets, until their depletion, and interval III, where polymerization continues within the particles until the monomer is consumed.

A three stage process also occurs in semibatch emulsion polymerization reactions: a batch period in which a small fraction of the total monomer amount is polymerized; an addition period in which the rest of the monomer is flowed into the reactor ("growth stage"); a postaddition period to allow for polymerization of residual monomer. After the first stage, particle nucleation may be complete or, in some conditions, nucleation can continue during the feeding period.[12] Deviations from this general scheme have been introduced, such as exclusion of the batch stage and addition of monomer "shots" instead of constant monomer feed.

*Corresponding author.

Semibatch emulsion polymerization processes are usually carried out using two different feed types: neat monomer feed,[13] where only monomer is flowed into reactor or monomer emulsion feed,[14] in which aqueous emulsifier is added with the monomer. The systems for which a critical flow rate has been reached such that the rate of polymerization is controlled by the rate of monomer addition, are called "starved".[15] In this case, there are no more monomer droplets and the monomer concentration in the polymer particles is lower than the saturated concentration. If the feed rate is higher than the polymerization rate, the monomer accumulates in the reactor as monomer droplets. This is usually termed a "flooded" system. In a flooded process, the particles are completely saturated with monomer and reaction kinetics resemble those of a batch emulsion polymerization, where particle growth rate is maximum and hence, particle nucleation is minimum. In the case of the semicontinuous emulsion polymerization, a maximum growth rate is obtained under monomer-flooded conditions, whereas the polymerization under monomer-starved conditions slows down particle growth rate and leads to a larger number of smaller particles.

Online monitoring of different emulsion characteristics, such as conversion, comonomer composition and particle size have been reported in numerous studies.[16−21] There is much less work, however, on assessing and controlling polymer molecular weight,[22−25] which in all studies reported so far is measured offline. Challenging issues are imposed by the complex nature of the systems studied and the difficulty of online measurements. Other phenomena such as chain transfer to polymer make the online control of the molecular weight distribution (MWD) more challenging.[26,27] Reaction calorimetry, oftentimes used due to the exothermicity of the emulsion polymerizations, does not provide a direct estimation of the unreacted monomer and state observers have to be used. The accuracy of the method is limited especially if

© 2009 American Chemical Society
Published on Web 10/14/2009

**Table 1. List of Experiments and Their Conditions**[a]

| | | | | MMA flow 1st stage | | MMA flow 2nd stage | | | | | |
|---|---|---|---|---|---|---|---|---|---|---|---|
| exp | type | $C_{MMA,0}$ (M) | $C_{m,ss}$ (g/mL) | rate (mL/min) | $\Delta t$ (min) | rate (mL/min) | $\Delta t$ (min) | latex $D_h$.[b] (nm) | polymer $M_{w,final\text{ACOMP}}$ (g/mol) | polymer $M_{w,final\text{SEC}}$ (g/mol) | polymer $\eta_{w\text{ACOMP}}$ (cm$^3$/g) |
| A1 | slow ramp | 0.04 | 0.0037 | 0.05 | 400 | | | 27 | $2.20 \times 10^5$ | $2.24 \times 10^5$ | NA |
| A2 | slow ramp | 0.04 | 0.0074 | 0.1 | 188 | | | 30 | $3.50 \times 10^5$ | $3.40 \times 10^5$ | 90 |
| A3 | fast ramp | 0.04 | 0.0288 | 0.4 | 60 | | | 40 | $7.50 \times 10^5$ | $1.00 \times 10^6$ | 150 |
| A4 | batch | 2.00 | NA | | | | | 80 | $2.80 \times 10^6$ | $4.20 \times 10^6$ | 530 |
| A5 | two-stage ramp | 0.04 | 0.0077 1st stage 0.1340 2nd stage | 0.1 | 106 | 2 | 6 | 22/32 | $3.20 \times 10^5$/ $1.22 \times 10^6$ | $3.70 \times 10^5$ / $1.16 \times 10^6$ | 85/140 |
| A6 | one shot MMA | 0.04 | 0.0074 | 0.1 | 36 | 17 mL one shot | | 20/50 | $2.25 \times 10^5$/ $1.35 \times 10^6$ | $3.16 \times 10^5$/ $3.00 \times 10^6$ | 80/170 |
| A7 | high $C_{MMA,0}$ | 0.30 | 0.0074 | 0.1 | 204 | | | 42.5 | $5.04 \times 10^5$ | $5.58 \times 10^5$ | 75 |

[a] All the reactions were done at 70 °C and were initiated by KPS, whose concentration was 4.8 mM. In all reactions $c_{SDS,0}$ was $5 \times 10^{-3}$ g/cm$^3$, and the reactor was fed from a reservoir of bulk MMA (0.936 g/cm$^3$). $C_{MMA,0}$ = concentration before starting to flow more monomer; all concentrations in reactor. $C_{m,ss}$ = monomer concentration when steady state is reached. Note. $\alpha = 0.0021\ s^{-1}$ is the reaction rate coefficient from the batch reaction, used in the analysis of all the subsequent semi-batch reactions. [b] $D_h$ values at the end of monomer flow.

applied in semicontinuous processes under starved conditions. Online viscometry and UV monitoring offered alternative routes in evaluating polymer mass by viscosity during polymerization in inverse emulsion.[28] Spectroscopic techniques provide a more direct measurement of the monomer conversion. NIR[29] and photon correlation spectroscopy were used to estimate monomer concentrations and particle size of polymer emulsions.[30] Well-defined MWD polymers were obtained by means of control strategies based on online gas chromatography (GC) measurements.[31] However, the lack of robustness of the sampling/dilution employed makes GC currently unfeasible for industrial implementation. Recently, the authors reported the online determination of MWD by coupling for the first time automated multidetector size-exclusion chromatography (SEC) with the continuous nonchromatographic based ACOMP method to obtaining $M_w$.[32] The chromatographic addition is most useful when reactions are slow (there is typically a 10 min interval between discrete, automatic SEC measurements) and detailed knowledge of the MWD is required (e.g., for "living" type reactions).

Most of the monitoring methods reported are focused on a single feature of the process studied. A recently developed methodology[33] allowed simultaneous characterization of the polymer/monomer components (continuous determination of $M_w$, reactions kinetics, average composition distribution, etc.) and the colloidal components; monomer droplets and polymer latex particles during the online monitoring of the reactions.

In most of the studies mentioned above, estimation of reaction kinetics requires calibration models and algorithms to be used, which have to account for all the effects of competing events, such as particle nucleation, which for more hydrophilic monomers is important, coagulation, monomer droplets, changes in concentrations, etc. A large drawback of the *in situ* methods is that they work in concentrated reaction environments, and hence the signals obtained usually must be interpreted using chemometric or other empirical calibration schemes. Furthermore, such probes are easily fouled or damaged by the reaction environment, causing large shifts of the empirical calibration schemes. In contrast, the online method presented here provides, through the ACOMP "front-end" comprising an ensemble of pumps, dilution and conditioning stages, a continuous, dilute, and well conditioned sample stream to the sensitive detector train, and allows model-independent quantities such as conversion, composition and molar mass distribution, to be determined.

Particular emphasis is given in this work to the methodology used to monitor molecular weight evolution during the reaction, in an absolute fashion, based only on multiangle light scattering detection and with no need to use any models concerning the reaction steps or particular mechanisms. Likewise, the monomer and polymer concentration data are obtained purely from natural constants, i.e., the extinction coefficients of the various species, mass balance, and firm knowledge of semibatch pump rates, without need for modeling raw data according to hypothesized mechanisms. In this context, the method used here offers a significant advance not only because it provides means to immediately asses the regime the reaction occurs in but also allows verification of the effects of any change in the monomer feed rates on key parameters during the synthesis.

In the present work, the ACOMP technique was used to quantify in a novel manner different aspects of the reaction kinetics in semicontinuous mode are presented here. The semibatch emulsion polymerization of methyl methacrylate (MMA) at 70 °C under different reaction regimes such as monomer-starved and monomer flooded conditions was chosen as a case study.

## Experimental Section

The polymerization reactions were performed in a 150 mL three-neck round-bottom flask reactor equipped with a condenser, under magnetic stirring. The initial volume of reactor fluid was 100 mL in each experiment. Nitrogen was flowed before and throughout the reactions. All the materials, methyl methacrylate (MMA), tetrahydrofuran (THF) potassium persulfate (KPS), and sodium dodecyl sulfate (SDS), were used as received from Aldrich. Milli-Q deionized water, filtered through a 0.22 $\mu$m filter, was used during the polymerization reactions and for the preparation of the samples in the subsequent measurements.

Typically, after the solvent baseline was stabilized, continuous withdrawal/dilution with THF of the reactor content started and allowed monomer baseline to be obtained. It was recently shown that complete dissolution of the reactor emulsion with THF occurs within tens of seconds, producing a continuous, homogeneous, dilute solution that makes possible online measurements of monomer/polymer properties.[33] As the temperature reached the preset value (70 °C), KPS was added and the flow of the rest of the monomer into the reactor started. The monomer added to the reactor was from a reservoir of bulk MMA at 25 °C, under $N_2$. In addition to the continuous monitoring, discrete aliquots were manually withdrawn from the reactor for subsequent multidetector size exclusion chromatography and dynamic light scattering measurements.

Polymerization reactions were performed with monomer feed rates targeted to produce desired effects. The experiments, their flow rates and other conditions are listed in Table 1. In the so-called monomer-starved conditions, the rate limiting step for polymerization is the rate at which monomer is fed into the reactor. The experiments explore the effects on reaction kinetics, $M_w$ and particle properties by the use of two strategies: varying monomer feed while the reaction occurs in the starved regime,

and by suddenly "flooding" the reaction with monomer, using different flow schemes. A batch polymerization (A4) was also carried out to provide a benchmark for the inherent polymerization rate coefficient of the reaction. The first order rate coefficient under the conditions used here ($\alpha$, as defined below) was 0.0021 $s^{-1}$.

**Techniques.** *ACOMP*. A small stream was continuously extracted from the reactor, at a rate of 0.06 mL/min in all reactions, via a Fluid Metering Q pump, diluted with THF by a factor of 34 in a first low pressure mixing stage, then by an additional factor of 9 in a second low pressure stage for a total dilution of 309x. This hence yielded a dilute solution in the range of ($1.3 \times 10^{-5}$ to $6.5 \times 10^{-4}$) g/$cm^3$ combined polymer and monomer concentration. The reactor emulsion diluted with THF was passed through detectors at 1 mL/min during the reaction and data was collected every two seconds, with a 15 min lag time between reactor extraction and detector measurements

A 2 $\mu$m inline frit was included between the final pump and the detector train, consisting of a custom-built single capillary viscometer, a Waters 410 refractive index detector (RI), a Brookhaven Instruments Corporation BI-$M_w$A multiangle light scattering (MALLS) detector, and a Shimadzu Corporation SPD-M20A photodiode array detector (UV).

*Size Exclusion Chromatography* (*SEC*). Multidetector SEC was used to measure MWD, different moments of the distribution, as well as $[\eta]_w$, radius of gyration, etc. Two PLgel MixedB chromatographic columns in series were used. THF was flowed using a Shimadzu HPLC pump through columns and detector train, comprising viscometer, MALLS, RI, UV at 0.8 mL/min.

*Dynamic Light Scattering* (*DLS*). Particle size was measured offline using a Brookhaven 90-plus detector ($\lambda$ = 670 nm) operating at a scattering angle of 90°, at room temperature. Particle hydrodynamic diameter $D_h$ (the intensity-weighted average diameter) was determined based on the Stokes−Einstein equation. The samples withdrawn from the reactor were diluted with water for these measurements to be made. Online monitoring of the particle size and distribution was not possible here due to the small latex particles produced (below the detection limit of the Mie scattering particle size detector). Kind donation of a Brookhaven Instruments Nano-DLS detector allows the simultaneous monitoring of polymer and particle properties in future work.

**Discussion on Reaction Kinetics.** All the reactions in Table 1 were carried out at $T$ = 70 °C with the same concentration of initiator, KPS. The half-life of KPS is 20.86 h at 70 °C so the number of the radicals was constant throughout the reaction. Hence, $\alpha$ is the same for all reactions in Table 1, which simplifies kinetic comparisons among the experiments.

During the reaction, the mass of monomer in the reactor, $m(t)$ is given by the mass balance equation that relates monomer and polymer mass via

$$m(t) = m_{tot}(t) - m_p(t) \tag{1}$$

where $m_p(t)$ is the polymer mass in the reactor

If monomer is fed into the reactor at constant flow rate, $r_{add}$ ($cm^3$/s) from a reservoir of monomer concentration $c_{m,f}$, and reactor fluid is extracted from the reactor at rate $r_{ex}$ ($cm^3$/s) for the ACOMP stream, then the total amount of monomer plus polymer in the reactor at time $t$, $m_{tot}$ ($t$) is the sum of all monomer pumped into the reactor, the amount of monomer/polymer extracted plus any initial monomer present in the reactor. On the basis of the equation above, this has been shown[34] to be given by

$$m_{tot}(t) = \frac{m_0}{\left(1 + \frac{(r_{add} - r_{ex})}{V_0} t\right)^{r_{ex}/(r_{add} - r_{ex})}} + r_{add} c_{m,f} t \tag{2}$$

where $m_0$ is the initial mass of monomer in the reactor and $V_0$ is the initial volume of liquid in the reactor.

Now, to take into account the time effects of both the polymerization kinetics and the flow of monomer into the reactor, batch expressions for first order monomer conversion are combined with those for reagent mass balance when reagents are flowed into a reactor, such as eq 2. In this case, the monomer concentration, [M]($t$) at any time becomes

$$[M](t) = [M]_0 \exp\left\{-\left(\frac{r_{add} + \alpha V_0}{V_0}\right) t\right\} + \left(\frac{[M]_f r_{add}}{r_{add} + \alpha V_0}\right)\left(1 - \exp\left\{-\left(\frac{r_{add} + \alpha V_0}{V_0}\right) t\right\}\right) \tag{3}$$

where $[M]_0$ is the initial monomer concentration in the reactor, $[M]_f$ is the concentration of bulk MMA fed in the reactor, and $\alpha$ is the first-order reaction rate coefficient.

The rate of polymerization, $R_p$ is independent of $r_{add}$ as long as $r_{add}$ is large enough to maintain the saturation value of the monomer concentration $[M]_{p,sat}$ in the latex particles. If [M] decreases below this value, a steady state is reached, and $R_p$ approaches $r_{add}$.

In an emulsion reaction the monomer is partitioned between particles/droplets and aqueous phase. At higher concentration, no more monomer dissolves in water and the excess separates into droplet phase. The following empirical equation[35]

$$[M]_{aq} = [M]_{aq,sat} \frac{[M]_p}{[M]_{p,sat}} \tag{4}$$

was used to correlate the monomer concentration in the aqueous phase, $[M]_{aq}$ to that in the polymer phase, $[M]_p$. $[M]_{p,sat}$ = 6.6 M and $[M]_{aq,sat}$ = 0.15 M are the corresponding saturation values from the literature.[36,37]

Equation 3 predicts that no matter what the initial concentration $[M]_0$ in the reactor, a quasi-steady state will be reached, with an e-fold period of $V_0/(r_{add} + \alpha V_0)$. The steady-state concentration finally reached in any case is

$$[M]_{ss} = \left(\frac{[M]_f r_{add}}{r_{add} + \alpha V_0}\right) \tag{5}$$

This means that the steady state polymerization rate, $R_{p,ss}$ will be given by

$$R_{p,ss} = \alpha\left(\frac{[M]_f r_{add}}{r_{add} + \alpha V_0}\right) \tag{6}$$

This is in agreement with the literature.[15,38]

$$\frac{1}{R_p} = \frac{1}{K} + \frac{1}{r_{add}} \tag{7}$$

where $K$ is a parameter that indicates of the process capability to consume monomer and depends on variables such as initiator, surfactant concentrations, temperature. As $K$ increases, $R_p$ approaches the rate of monomer addition, indicating a higher steady-state rate of reaction at a fixed $r_{add}$. Examination of the reciprocal of eq 5 allows the constant $K$ to be identified via

$$\frac{1}{R_{p,ss}} = \frac{1}{\alpha[M]_f} + \frac{V_0}{r_{add}[M]_f} \tag{8}$$

as $K = \alpha[M]_f$.

In keeping with standard semibatch definitions, the instantaneous conversion $f_{inst}$ is defined as the total mass of polymer in

the reactor divided by the total mass of monomer in the reactor (feed + initial charge) at the time $t$:

$$f_{inst}(t) = \frac{m_{tot}(t) - m(t)}{m_{tot}(t)} \tag{9}$$

Using this definition, together with eqs 1, 2 for $m_{tot}(t)$ and $m(t)$ yields

$$f_{inst}(t) = 1 - V(t)\frac{c_{m,0}\exp\left\{-\left(\frac{r_{add}+\alpha V_0}{V_0}\right)t\right\} + \left(\frac{[m]_f r_{add}}{r_{add}+\alpha V_0}\right)\left(1-\exp\left\{-\left(\frac{r_{add}+\alpha V_0}{V_0}\right)t\right\}\right)}{\frac{m_0}{\left(1+\frac{(r_{add}-r_{ex})}{V_0}t\right)^{r_{ex}/(r_{add}-r_{ex})}} + r_{add}c_{m,f}t} \tag{10}$$

The overall or total conversion, $f_{tot}$, is defined as the as the ratio of the polymer in the reactor to the total monomer in the recipe.

$$f_{tot} = \frac{[M]_0 - [M](t)}{[M]_0} \tag{11}$$

The polymer concentration $c_p$ must be known in order to compute $M_w$ and $[\eta]_w$ from the raw light scattering and viscosity data. In the case of semibatch reactions, $c_p(t)$ can be computed from mass balance and it can be shown to be

$$c_p(t) = \frac{1}{V(t)}\left\{\frac{m_0}{\left[1+\frac{r_{add}-r_{ex}}{V_0}t\right]^{r_{ex}/(r_{add}-r_{ex})}} + r_{add}c_{m,f}t\right\} - \left\{c_{m,0}e^{-\beta t} + \frac{r_{add}c_{m,f}}{r_{add}+\alpha V_0}(1-e^{-\beta t})\right\} \tag{12}$$

The right-hand term on the right-hand side is a transient that dies away with the characteristic rate

$$\beta = \frac{r_{add}+\alpha V_0}{V_0} \tag{13}$$

In this work, $\alpha V_0 = (0.0021\ s^{-1}) \times 100\ cm^3 = 0.21\ cm^3/s$. Comparison with the monomer flow rates into the reactor is given in Table 1, $\alpha V_0 \gg r_{add}$ for all experiments. The typical $r_{add}$ was 0.0017 $cm^3/s$, and the maximum value of $r_{add}$ was 0.033 $cm^3/s$, in the second feed stage of A5. Hence, $\beta \sim \alpha$ for conditions in this work.

Furthermore, in this work the semibatch feeds typically lasted much longer than $1/\beta$ (500 s). Also $V(t)$ did not change by a large amount, typically less than 10% in all experiments, except for A3, where the volume increased by 20% by the end of the reaction. In this case, $c_p(t)$ becomes approximately linear for $t \gg 1/\beta$, according to

$$c_p(t) \approx c_{m,0} + \rho c_{m,f}t/V_0 \tag{14}$$

The computed polymer concentrations are used to determine cumulative weight-average molecular mass $M_w$, second virial coefficient $A_2$ and the $z$-averaged mean square radius of gyration $< S^2 >_z$, based on Zimm approximation ($q^2\langle S^2\rangle_z \ll 1$)

$$\frac{Kc}{I(q,c)} = \frac{1}{M_w}\left(1 + \frac{q^2\langle S^2\rangle_z}{3}\right) + 2A_2c \tag{15}$$

where $K$ is an optical constant ($= 4\pi^2 n^2 (dn/dc)^2/N_A\lambda^4$, for vertically polarized incident light), $n$ is the solvent index of refraction, $q$ is the scattering wave-vector, $\lambda$ is the vacuum wavelength of the incident light, and $dn/dc$ is the polymer incremental index of refraction. It is important to note that within the limit of approximation of eq 15, there are no assumptions about particle shape or morphology and thus it can be used for random coils, cross-linked, branched, rodlike polymers, etc.

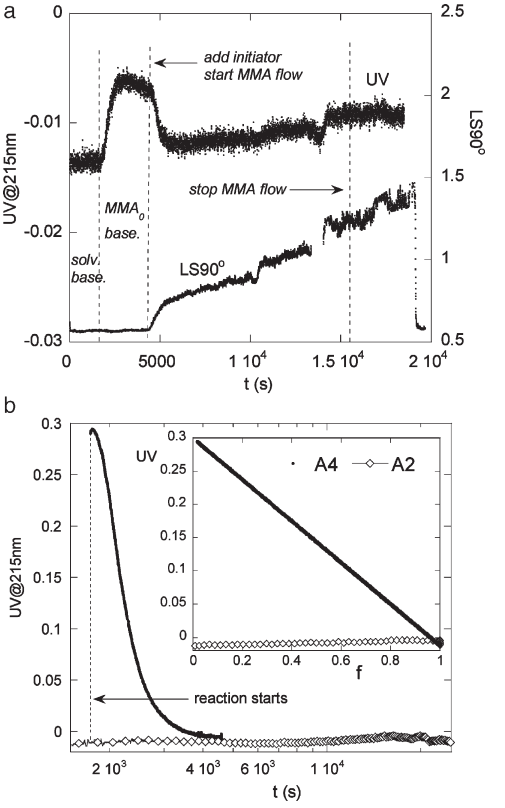


**Figure 1.** (a) Raw ACOMP data: light scattering (90°) and UV signals during a semibatch reaction (A7). (b) UV data from reactions in monomer starved conditions (A2) vs flooded conditions (A4).

It can be valuable to use $M_w(t)$ from the light scattering data to compute $M_{w,inst}(t)$ for predicting values of $M_w(t)$, which is what the multiangle light scattering in ACOMP measures directly.

Finally, the use of the computed polymer concentrations together with the continuously measured viscosity data allows reduced viscosity, $\eta_w$ to be determined.

## Results

Results from all polymerization reactions made, in terms of both polymer and latex properties, are listed in Table 1.

Shown in Figure 1a are raw light scattering at 90° and UV data from a semibatch reaction (A7). This is a case in which the transition from flooded conditions (higher initial monomer amount in the reactor) to monomer starved conditions (low feed rate) occurred; $c_m$ in the reactor fell from an initial value of 0.030 $g/cm^3$ to its steady state value of 0.0078 $g/cm^3$, with a first order (exponential) rate coefficient of 0.0022 $s^{-1}$, obtained by an exponential fit to the UV data at 215 nm. This value is very close to $\beta \cong \alpha = 0.0021\ s^{-1}$. This is the value predicted above for the time to reach the steady state, according to eq 5.

The UV absorbance is given at any time by the sum of the signals from each species

$$V_{UV} = (\varepsilon_m c_m(t) + \varepsilon_p c_p(t))l$$

where $l$ is the path length of the UV cell, $c_m$ and $c_p$ are the mass concentrations of the monomer and polymer, respectively,

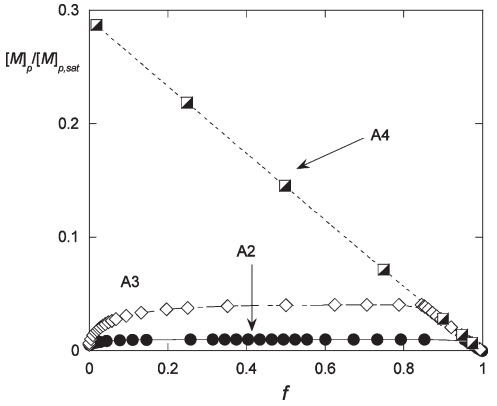


**Figure 2.** Computed $[M]_p/[M]_{p,sat}$ behavior during batch (A4) and semibatch reactions (A2 and A3) as a clear indicator of the regime each reaction occurs.

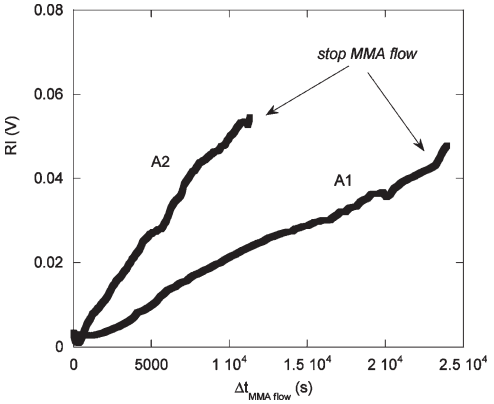


**Figure 3.** RI signals for reactions A1 and A2. The time has been set to $t = 0$ for the start of the reaction for graphical ease of comparison.

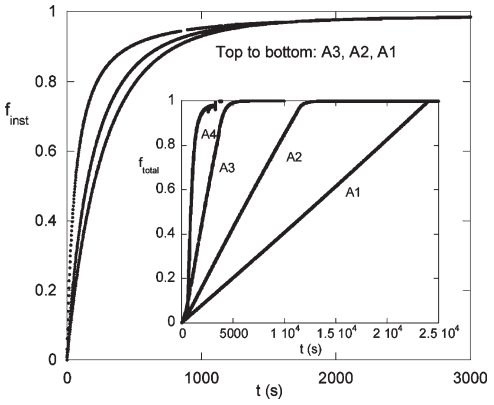


**Figure 4.** Instantaneous conversion curves as functions of time for A1−A3 semibatch reactions with different monomer addition rates. In the inset: total monomer conversion for the same reactions together with data from a batch reaction, A4, for comparison.

$\varepsilon_m$ and $\varepsilon_p$ are extinction coefficients, the latter being negligible in this case since the polymer does not have a significant contribution to the total UV absorbance. Generally, in a batch reaction, once the reaction begins, the UV decreases as the monomer is consumed and loses the double bond. In fact, the UV signal provides the definitive indication that the reaction falls from the "flooded" condition to the steady state, or "starved" condition. Thus, as shown in the figure, the UV signal falls to a fairly constant value, almost at the solvent baseline value, with a subsequent slow increase as the reaction progresses due to a small amount of scattering by the increasing amount of polymer. Light scattering steadily increases throughout the reaction indicating the polymer production. The initial rapid rise around 5000s corresponds to the large $M_w$ chains produced at the outset of the reaction, typical of free radical polymerization.

The use of the continuous monitoring of the UV signals as a robust means of determining whether a reaction is in the starved or flooded regime is exemplified in Figure 1b for experiments A2 and A4. UV data at 215 nm are represented vs time, and vs total monomer conversion, in the inset, respectively. The signals clearly show the difference between the regimes under which the reactions occur: flooded, high amplitude and fast kinetics, and starved, small UV due to the low amount of monomer and slow kinetics. In experiment A2, the low initial monomer concentration $c_{m,0} = 0.004$ g/cm$^3$ (at steady state, $c_{m,ss} = 0.078$ g/cm$^3$) gives, after 309× dilution, negligibly small UV signal, which does not build, indicating that all monomer is polymerized at the rate it is fed into reactor and does not accumulate. On the other hand, for the batch reaction A4, a much higher magnitude of the UV signal is observed ($c_{m,0} = 0.200$ g/cm$^3$), which subsequently decreases following a first order decay as the monomer is consumed. The total amount of monomer converted in both reactions was similar, ∼20 g. It should also be noted that the time scale in the figure is logarithmic, since the batch reaction has a 500 s reaction e-fold, whereas the semibatch reaction continued for 30 000 s.

The UV signal is near the solvent baseline at the steady state for most of the reactions in Table 1. While the constancy of the UV proves that the steady state is reached, it does not provide a direct signal for computing conversion. It is possible to use equations presented in the previous section to compute $c_m(t)$ and $c_p(t)$, given that the flow rates are well-known.

The computed monomer concentrations together with eq 4 were used furthermore to estimate the evolution of the monomer concentration within the particles, $[M]_p$ during the reactions. As an alternative way to show the difference between the flooded and starved regimes, the ratio $[M]_p/[M]_{ps}$ is illustrated in Figure 2 for two reactions in semicontinuous mode (A2 and A3) and for a batch reaction (A4). Monomer starved conditions prevail for the semibatch reactions, where the ratio$[M]_p/[M]_{p,sat}$ is very low (increasing with the rate of addition, as expected) and contrasts to the values computed for the batch reaction where $[M]_p/[M]_{p,sat}$ starts at 0.3, under monomer saturation conditions and decreases with conversion as the monomer is consumed.

The RI signals are an interesting adjunct to the UV and LS signals, in that they mainly provide a direct measure of $c_p$. Figure 3 shows RI signals for reactions A1 and A2 during the time monomer was pumped into the reactor. The time axis has been set to $t = 0$ for the start of the reaction for graphical ease of comparison. The differential refractive index increments, d$n$/d$c$, for MMA and pMMA in THF are 0.02 and 0.10, respectively so that the RI response is biased toward polymer concentration. The salient feature is that the RI signal is fairly linear throughout the course of the reaction. As the steady state is reached (after ∼ 500s in this work), $c_p$ should increase linearly, since $R_p$ is constant, as long as $[R\cdot]$ remains constant and $c_m$ should be small and constant. Hence, the RI should respond linearly. The conversion process and the near-linear nature vs $t$ are confirmed in the examples shown in the figure.

**Effect of Monomer Feed Rate on the Reaction Rate.** Shown in Figure 4 are instantaneous conversion curves for experiments A1−A3, semibatch reactions with different monomer addition rates, $r_{add}$, computed via eq 10. As illustrated in the figure, $f_{inst}$ increases rapidly and reaches high values in relatively short times. In the inset, total conversion curves are shown as functions of time for the same reactions. Data from a batch reaction, A4, determined directly from the UV signal at 215 nm is also shown in the inset for comparison.

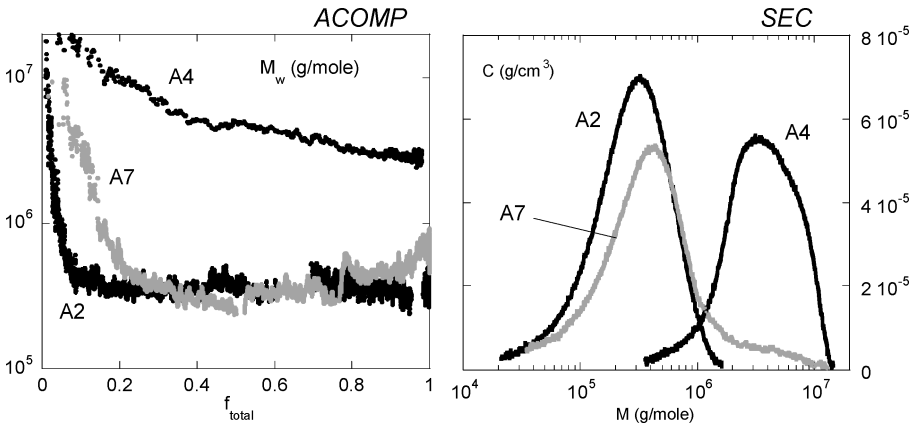


**Figure 5.** Effect of the monomer feed rate on $M_w$ for experiments A2, A4, and A7 (left panel) and mass distributions for the same experiments, as determined from SEC (right panel).

The rate of polymerization increased with $r_{add}$. At higher feed rates, more monomer accumulates in the reactor and the rate of polymerization approaches that of batch polymerization.

**Effect of the Feed Rate on the Polymer Molecular Weight.** Polymer molecular weight plays an important role in defining the macroscopic characteristics and material performance of the reaction endproduct. The rate of monomer addition has a large impact on the polymer molecular mass and on the MWD. As found in other studies,[17,38,40] the highest $M_w$ values are obtained for the polymers synthesized during batch reactions. In the case of the semibatch reactions, the molecular weight of the polymer decreases with the decrease in the monomer feed rate, under the studied conditions.

Unlike in most of the studies reported, in this work $M_w$ was determined during the online monitoring of the polymerization and in an absolute fashion, based on the multiangle light scattering detection available. This is a remarkable feature of this work because it eliminates the use of any model in computing the polymer mass. Continuous measurement of $M_w$ of fully solubilized, unentangled polymer chains by ACOMP was possible due to the rapid and complete dissolution of the reactor emulsion into a homogeneous solution in THF (tens of seconds).[33] Light scattering detection was also used in SEC, rather than any column calibration using molecular weight standards.

Shown in Figure 5, left panel, are $M_w$ curves as functions of total conversion for three selected reactions with the same solid contents but different monomer feed schemes from ACOMP (left panel) and MWDs from SEC for the same experiments (right panel). Both techniques capture distinct $M_w$ kinetics as the transition from monomer flooded to starved conditions is monitored (experiment A7), which are compared to those for a batch reaction (experiment A4) and for a reaction in starved conditions (experiment A2). Typical free radical behavior is observed for the $M_w$ trend in A4, where $M_w$ decreases with conversion since longer chains are being formed at the beginning, followed by shorter chains produced as the reaction progresses. In contrast, for A2 and A4 experiments, made in semibatch conditions, $M_w$ reaches a plateau around 20% conversion and shows much smaller magnitude compared to the polymer mass produced in batch conditions. The monomer flow rate into the reactor was the same for A2 and A7 and so $M_w$ reaches the same level at steady state. Since A7 began with a higher concentration of monomer initially in the reactor, however, it takes longer to achieve the $M_w$ plateau than A2, where it is recalled that the $M_w$ is the cumulative value in the reactor at each moment.

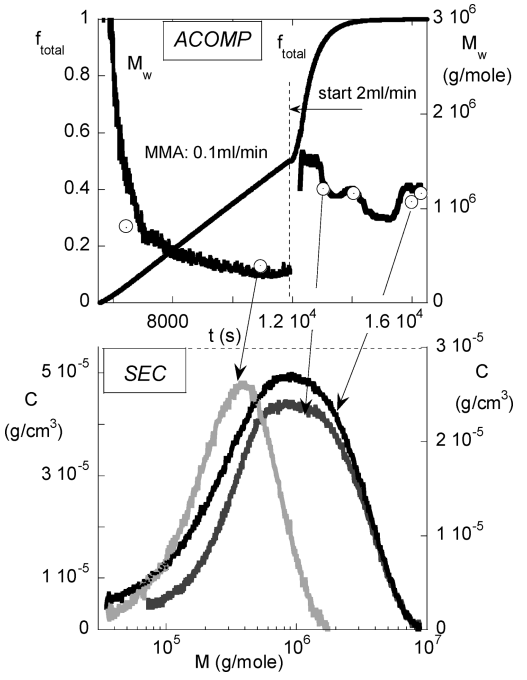


**Figure 6.** Hybrid behavior of $M_w$: $M_w$ from ACOMP data for A5 together with selected SEC mass distributions.

The shape and breadth of the MWD provided by SEC is also affected by the details of monomer addition, e.g., A7 shows right skew of $M_w$ from its relatively high initial monomer concentration followed by a majority of monomer fed at low rate. A2, where almost all monomer is flowed in shows the most symmetrical MWD. The batch reaction, A4 shows asymmetry due to much of the very large polymer coming out in the exclusion volume, which distorts the chromatogram

An interesting $M_w$ trend is achieved during the semibatch reaction A5, shown in Figure 6. This is an example of a "hybrid" reaction, where the polymer mass increases 1 order of magnitude as the transition from monomer starved to monomer flooded condition is made by the increase in the rate of monomer addition from 0.1 mL/min to 2 mL/min around 50% total conversion. Selected SEC chromatograms corroborated with ACOMP data show in their shape and breadth how the MWD is also affected by the details of monomer addition and follows the transition from low to higher molecular weight polymer. Smaller polymer mass was

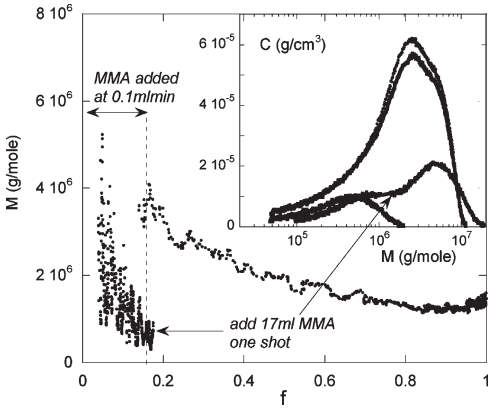


**Figure 7.** Hybrid behavior of $M_w$: from ACOMP data for A6 together with selected SEC mass distributions.

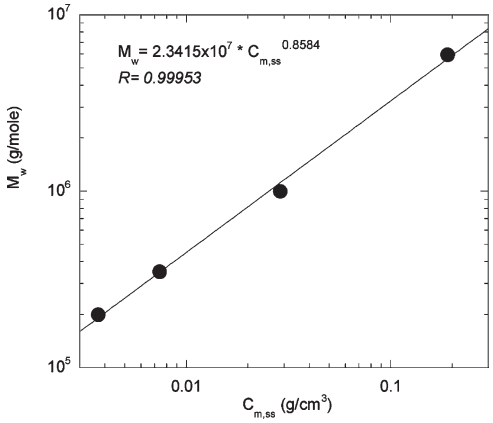


**Figure 8.** $M_w$ vs $C_{m,ss}$ for experiments A1-A4. The A4 data are taken as the $M_w$ value near the beginning of the reaction when the QSSA plateau is reached.

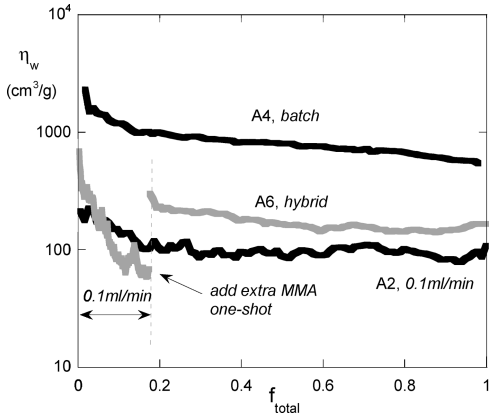


**Figure 9.** Effect of the monomer feed rate on $\eta_w$: $\eta_w$ data from experiments A2, A4, and A6 are as functions of time.

obtained during the slow monomer feed stage, followed by a jump in $M_w$ as the rate of monomer addition was increased, after flooded conditions dominate the reaction kinetics.

The change in the monomer feed rates during reactions allowed simultaneous influence and verification of the evolution of these parameters during the synthesis. The adjustable feed rate confers great power for controlling $M_w$ during the reaction.

Thus, the second "hybrid" reaction, A6, starts in semicontinuous mode, under starved conditions, achieved by slow monomer feed in the reactor, and becomes essentially a batch reaction upon the one-shot addition of MMA at 15% conversion. The transition from monomer starved to monomer flooded conditions followed by ACOMP is shown in Figure 7, in which reaction kinetics were changed in an earlier stage than in A5, by the addition of the monomer shot. Continuous $M_w$ results from ACOMP corroborated by SEC discrete points follow the evolution from low to high molecular weight polymer produced by the extra-MMA addition. This is marked by the buildup of a high molecular weight shoulder in the corresponding SEC mass distribution. It was again found that the conversion rate after the flooding event was close to the value α, since the reaction kinetics in this stage follow the batch reaction kinetics.

The effect of the flow rate on the evolution of $M_w$ can be anticipated from eq 5 for the steady state monomer concentration $c_{m,ss}$, which according to eq 7, is proportional to $r_{add}/(r_{add}+\alpha V_0)$. $M_n$ will be directly proportional to $c_{m,ss}$ for a given value of α, if $k_p$ and $k_t$ are the same and there is no chain transfer. There has been no evidence for any significant chain transfer for MMA bulk reactions and the $M_w$ vs $f$ profile for the batch reaction A4 also does not show evidence for chain transfer (Figure 5). Since α is the same for all reactions here, it would be expected that the steady state value of $M_w$ should be proportional to $c_{m,ss}$ and hence also approximately proportional to flow rate. Figure 8 shows the final $M_w$ vs $c_{m,ss}$ which has a power law of 0.86, which, although not quite linear, shows a strongly increasing $M_w$ with flow rate and $c_{m,ss}$. The deviation may be at least partly related to a chain length and concentration dependence of $k_t$ and $k_p$.[39−44] The A4 data are taken as the $M_w$ value near the beginning of the reaction when the QSSA plateau is reached.

Reduced viscosity, $\eta_w$ was also affected by the changes in the monomer feed rates, from a reaction to another and during the same reaction. A similar behavior to the $M_w$ trends was observed in the case of the semibatch reactions, $\eta_w$ decreases with the decrease in the monomer feed rate, under the studied conditions. Figure 9 shows $\eta_w$ for selected experiments (A2, A4, and A6), with different flow schemes. As expected, polymer from the reaction in batch A4 shows the highest viscosity, compared to the ones produced under semibatch conditions. Moreover, the transition in the reaction regime, produced by the addition in one shot of MMA in the case of experiment A6 is captured by the jump in the $\eta_w$, which almost doubles its value. The $\eta_w$ values at final conversion or, when appropriate, at the end of a flow stage, are listed in Table 1.

**Effect of Monomer Feed Rate on the Particle Size and Number.** Particle size was measured offline using a Brookhaven detector ($\lambda$ = 670 nm) operating at 90°, at room temperature. In all the semibatch reactions, regardless of the flow rates used during the monomer addition, a gradual increase of the particle size is noticed. The particle hydrodynamic diameter values ($D_h$) at the end of the monomer feed stage are listed in Table 1. Generally, in the case of the semibatch reactions, the particle size was proportional to the rate of monomer addition, smaller particles being produced at low flow rate. In the case of the hybrid reactions, A5 and A6, the particle size and its subsequent increase depend on both initial conditions and on the conditions in which the second addition of the monomer was made. The extent of increase in the particle size after nucleation depends on the number of particles in the latex.

Shown in Figure 10 are DLS results on particle size for selected experiments. Smaller $D_h$ values are obtained for A2 and A3 experiments, where the monomer was added continuously, compared to $D_h$ for the latex particles produced during the batch reaction A4. The evolution of the particle

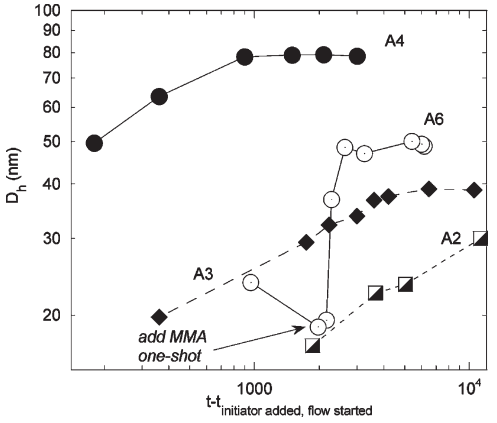


**Figure 10.** Effect of the flow rate on the evolution of the particle size. $D_h$ values for samples taken during reactions under different flow schemes (A2, A3, A4, and A6). The particles produced in batch are by far larger than the ones from the "hybrid" reaction.

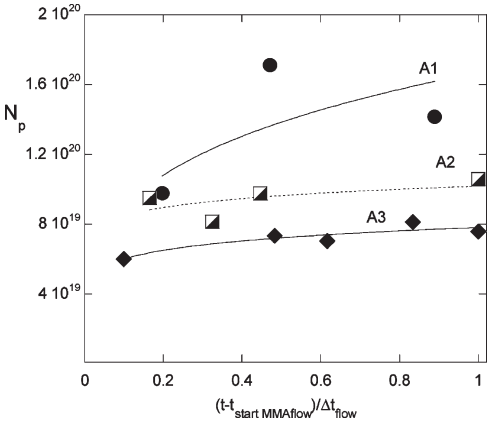


**Figure 11.** Evolution of the number of particles, $N_p$ during the semibatch reactions in which MMA was added in different flow rates.

size in a hybrid reaction (A6), in which most of the monomer was added in one shot after half an hour of monomer feed at 0.1 mL/min, was added to the figure. One could notice the effect of the continuous addition of the monomer in the first part of A6: the particles produced in batch are by far larger than the ones from the "hybrid" reaction. On the other hand, as the shot of MMA is added, typical batchwise behavior is achieved. A decrease in particle size at the addition of extra MMA is observed, due to further nucleation, followed by an increase as nucleation ceased. In the case of the reaction in batch, considered an equivalent to the semibatch one with a high rate of monomer addition, big particles are obtained from the beginning of the reaction because all were saturated with monomer during nucleation.

*Particle Number*. Typically, for the semibatch reactions, the number of particles increases at a lower rate of monomer addition. If monomer-starved conditions are achieved, particles are not saturated with monomer and grow at a rate controlled by the rate of monomer addition. In this case, the nucleation period is prolonged by a slower depletion of emulsifier micelles. Generally, for water-soluble monomers such as MMA, it is much easier to maintain starved conditions, because the formation of monomer droplets is delayed by the monomer dissolution in the water phase.

The number of particles was calculated using the following equation:

$$N_P = \frac{6mf_{inst}M_w}{\pi\rho_p D_v^3} \tag{16}$$

Here $D_v$ is the volume average diameter, $M_w$ is the monomer mass, $m$ is the mass of the monomer added into the reactor, and $\rho_p$ is the density of the polymer (1.178 g/cm$^3$).

Shown in Figure 11 is the evolution of the number of particles, $N_p$ calculated based on the above equation for experiments in which MMA was added at different flow rates. $N_p$ increases with the decrease in the rate of monomer addition. Also, $N_P$ should increases continuously with total conversion for all the addition rates studied here, more pronounced for slower monomer addition rate.

## Conclusions

Polymer molecular weight, $M_w$, reduced viscosity, $\eta_w$, and other kinetic parameters, such as conversion and monomer concentrations were monitored during semibatch emulsion polymerization reactions in which the monomer was introduced to the reaction sites with a rate depending on the rate of monomer addition. Kinetics for reactions in the monomer starved conditions were quantified. Additionally, interesting "hybrid" cases of transition between monomer flooded and starved modes due to change in monomer feed rates were studied, with marked and immediately monitorable changes in reaction characteristics. The effects of the type of the monomer addition on both polymer and latex characteristics were measured. Thus, lower monomer addition rates lead to a decrease in the polymer $M_w$ and $\eta_w$, and in the latex particle size but favors the increase in the number of the particles produced.

The use of the continuous monitoring of ACOMP signals offered a robust means of determining the characteristic features of the starved and flooded monomer conditions, and identifying them during the experiments, and also allowed the approach to the quasi-steady state to be monitored. The characteristic rate of the approach to the steady state after changing the flow rate was close to the batch rate coefficient for the experimental conditions in this work.

The successful ACOMP approach to monitoring semibatch polymerization reactions not only brings more complete and near-real time information about reaction mechanisms and kinetics, but also offers more accurate means to determine important reaction parameters, with subsequent possibilities for controlling and obtaining desired endproduct characteristics.

**Acknowledgment.** The authors acknowledge support from NSF CBET 0623531, Louisiana Board of Regents ITRS RD-B-5, Arkema, Inc., the Tulane Institute for Macromolecular Engineering and Science, NASA NNX08AP04A, and the Tulane Center for Polymer Reaction Monitoring and Characterization (PolyRMC).

## References and Notes

(1) Novak, R. W. *Adv. Org. Coat. Sci. Technol. Ser.* **1988**, *10*, 54–57.
(2) Chern, C. S.; Hsu, H.; Lin, F. Y. *J. Appl. Polym. Sci.* **1996**, *61*, 989–1001.
(3) Hergeth, W.-D., Online characterization methods, Wacker-Chemie GmbH, Burghausen, Germany: *NATO ASI Ser., Ser. E: Appl. Sci.* **1997**, *335*, 267−288.
(4) Dubé, M. A.; Soares, J. B. P.; Penlidis, A .; Hamielec, A. E. *Ind. Eng. Chem. Res.* **1997**, *36*, 966–1015.
(5) Sajjadi, S.; Brooks, B. W. *J. Appl. Polym. Sci.* **2001**, *79*, 582–597.
(6) Sajjadi, S. J. *J. Polym. Sci., Part A: Polym. Chem.* **2001**, *39*, 3940–3952.
(7) Plessis, C.; Arzamendi, G.; Leiza, J. R.; Schoonbrood, H. A. S.; Charmot, D.; Asua, J. M. *Ind. Eng. Chem. Res.* **2001**, *40*, 3883–3894.
(8) Sajjadi, S. *Langmuir* **2007**, *23*, 1018–1024.
(9) Elizalde, O.; Azpeitia, M.; Reis, M. M.; Asua, J. M.; Leiza, J. R. *Ind. Eng. Chem. Res.* **2005**, *44*, 7200–7207.

(10) Harkins, W. D. *J. Chem. Phys.* **1945**, *13*, 381–383.
(11) Smith, W. V.; Ewart, R. H. *J. Chem. Phys.* **1948**, *16*, 592–600.
(12) Sajjadi, S.; Brooks, B. W. *J. Appl. Polym. Sci.* **1999**, *74*, 3094–3110.
(13) Krackeler, J. J.; Naidus, H. *J. Polym. Sci. Part C: Polym. Symp.* **1969**, *27* (1), 207–235.
(14) Gerrens, H. *J Polym. Sci. Part C: Polym. Symp.* **1969**, *27* (1), 77–93.
(15) Wessling, R. A. *J. Appl. Polym. Sci.* **1968**, *12*, 309–319.
(16) Lau, W.; Westmoreland, D. G.; Novak, R. W. *Macromolecules* **1987**, *20*, 457–459.
(17) Lee, K. C.; El-Aasser, M. S.; Vanderhoff, J. W. *J. Appl. Polym. Sci.* **1992**, *45*, 2207–2219.
(18) Wu, X. Q.; Schork, F. J. *Ind. Eng. Chem. Res.* **2000**, *39*, 2855–2865.
(19) McCaffery, T. R.; Durant, Y. G. *Polym. React. Eng.* **2003**, *11*, 507–518.
(20) Reis, M. M.; Araujo, P. H. H.; Sayer, C.; Giudici, R. *Ind. Eng. Chem. Res.* **2004**, *43*, 7243–7250.
(21) Santos, A. F.; Lima, E. L.; Pinto, J. C.; Graillat, C.; McKenna, T. F. *J. Appl. Polym. Sci.* **2004**, *91*, 941–952.
(22) Ghielmi, A.; Storti, G.; Morbidelli, M.; Ray, W. H. *Macromolecules* **1998**, *31*, 7172–7186.
(23) Salazar, A.; Gugliotta, L. M.; Vega, J. R.; Meira, G. R. *Ind. Eng. Chem. Res.* **1998**, *37*, 3582–3591.
(24) Vicente, M.; BenAmor, S.; Gugliotta, L. M.; Leiza, J. R.; Asua, J. M. *Ind. Eng. Chem. Res.* **2001**, *40*, 218–227.
(25) Li, D.; Grady, M. C.; Hutchinson, R. A. *Ind. Eng. Chem. Res.* **2005**, *44*, 2506–2517.
(26) Britton, D.; Heatley, F.; Lovell, P. A. *Macromolecules* **2000**, *33*, 5048–5052.
(27) Vicente, M.; Leiza, J. R.; Asua, J. M. *Macromol. Symp.* **2002**, *182* (1), 291–303.
(28) Alb, A. M.; Farinato, F.; Calbick, J.; Reed, W. F. *Langmuir* **2006**, *22*, 831–840.
(29) Vieira, R. A. M.; Sayer, C.; Lima, E. L.; Pinto, J. C. *Ind. Eng. Chem. Res.* **2002**, *41*, 2915–2930.
(30) Reis, M. M.; Araújo, P. H. H.; Sayer, C.; Giudici, R. *Macromol. Rapid Commun.* **2003**, *24*, 620–624.
(31) Echevarria, A.; Leiza, J. R.; De La Cal, J. C.; Asua, J. M. *AIChE J.* **1998**, *44*, 1667–1679.
(32) Alb, A. M.; Drenski, M.; Reed, W. F. *J. Appl. Polym. Sci.* **2009**, *113* (1), 190–198.
(33) Alb, A. M.; Reed, W. F. *Macromolecules* **2008**, *41*, 2406–2414.
(34) Kreft, T.; Reed, W. F. *Eur. Polym. J.* **2009**, *45*, 2288–2303.
(35) Ballard, M. J.; Napper, D. H.; Gilbert, R. G. *J. Polym. Sci.: Polym. Chem. Ed.* **1984**, *22*, 3225–3253.
(36) Ledezma, R.; Treviño, M. E.; Elizalde, L. E.; Pérez-Carillo, L. A.; Mendizábal, E.; Puig, J. E.; López, R. G. *J. Polym. Sci.: Part A: Polym. Chem.* **2007**, *45*, 1463–1473.
(37) Liu, T.; Schuch, H.; Gerst, M.; Chu, B. *Macromolecules* **1999**, *32*, 6031–6042.
(38) Sajjadi, S.; Yianneskis, M. *Polym. React. Eng.* **2003**, *11*, 715–736.
(39) Zhu, S.; Hamielec, A. E. *Macromolecules* **1989**, *22*, 3093–3098.
(40) Mahabadi, H. K. *Macromolecules* **1985**, *18*, 1319–1324.
(41) Matsumoto, A.; Mizuta, K. *Macromolecules* **1994**, *27*, 5863–5870.
(42) Beuermann, S. *Macromolecules* **2002**, *35*, 9300–9305.
(43) Moad, G.; Moad, C. L. *Macromolecules* **1996**, *29*, 7727–7733.
(44) Olaj, O. F.; Vana, P.; Zoder, M. *Macromolecules* **2002**, *35*, 1208–1214.